Development of Lithium Chloride Absorber Radiator for Flight Demonstration

Michael G. Izenson[1], Scott D. Phillips[2], Ariane B. Chepko[3], and Gregory W. Daines[4]
Creare LLC, Hanover, NH, 03755

Gregory Quinn[5] and John Steele[6]
UTC Aerospace Systems, Windsor Locks, CT, 06096-1010

Water conservation is an essential requirement for future exploration spacesuits. Lithium Chloride Absorber Radiator (LCAR) technology has been developed to meet this requirement by rejecting heat without venting water from a Spacesuit Evaporator Absorber Radiator (SEAR) subsystem. Prototype LCARs have been developed and optimized through numerous thermal vacuum tests that simulate operation in space. An actual flight demonstration is a key next step needed to advance the technology readiness level of the LCAR and make it available for future exploration missions. This paper describes ongoing work to enable a flight test of an LCAR as part of a subscale SEAR system that uses an International Space Station (ISS) Extravehicular Mobility Unit (EMU) as a test bed. The twin goals of this program are to develop a prototype LCAR design that can integrate with an EMU using existing flight-qualified hardware, and to develop and demonstrate a regeneration system that is suitable for use on the ISS. Significant advances in LCAR technology include: (1) improved understanding of the thermodynamics of LiCl/water solutions and the way LiCl/water thermodynamics effect LCAR operation, (2) an optimized design of the absorber bed enables heat rejection at higher temperature and higher rates than prior LCAR designs, (3) measurement of improved heat rejection performance of the optimized LCAR panel through several absorption/regeneration cycles, (4) demonstration of a suitable coolant/refrigerant for use in the SEAR system, (5) demonstration that the prototype panel is extremely durable and maintains LiCl containment when tested against pressure and impact loads, and (6) demonstration that the LCAR's thermal performance is essentially unaffected after suffering a design-basis impact.

Nomenclature

ALCLR	=	Airlock Cooling Loop Recovery
EVA	=	Extravehicular Activity
EMU	=	Extravehicular Mobility Unit
ISS	=	International Space Station
LCVG	=	liquid cooling and ventilation garment
LCAR	=	Lithium Chloride Absorber/Radiator
LCG	=	Liquid Cooling Garment
MEOP	=	Maximum Expected Operating Pressure
NCG	=	Noncondensible gas
PLSS	=	Portable Life Support System
P-T	=	pressure-temperature
SEAR	=	Spacesuit Evaporator/Absorber/Radiator

[1] Principal Engineer, Creare LLC, mgizenson@creare.com.
[2] Engineer , Creare LLC, sxp@creare.com.
[3] Engineer, Creare LLC, abc@creare.com.
[4] Engineer, Creare LLC, gwd@creare.com.
[5] Staff Research Engineer, 1 Hamilton Road, Windsor Locks, CT 06096-1010/Mail Stop 1A-2-W66.
[6] Engineering Fellow, 1 Hamilton Road, Windsor Locks, CT 06096-1010/Mail Stop 1A-2-W66.

SWME = Spacesuit Water Membrane Evaporator
TRBF = Tile Repair Backpack Frame
UTAS = UTC Aerospace Systems

I. Introduction

Future space exploration missions will take astronauts far from Earth into extreme thermal environments, where temperature control of spacesuits will be a critical life support function. Existing thermal control technology relies on venting water to space to provide all or some of the required cooling. This approach is extremely costly, and possibly unsustainable, for future exploration missions. To enable frequent EVA without consuming large amounts of water, NASA, Creare, and UTC Aerospace Systems (UTAS) are developing Spacesuit Evaporator/Absorber/Radiator (SEAR) technology. Prior studies[1] have shown that adoption of SEAR technology has the potential to save thousands of kilograms of consumable water mass.

The main components of a SEAR system are the LiCl Absorber Radiator (LCAR)[2,3] and the Space Water Membrane Evaporator (SWME)[4,5] (Figure 1). The SWME absorbs heat generated inside the spacesuit by evaporating water through a bundle of porous hollow fibers. The LCAR comprises an array of radiator panels that also provide external structure for the PLSS (Portable Life Support System) backpack. Each LCAR panel contains a LiCl/water solution that absorbs the water vapor generated by the SWME and radiates heat to the environment at high temperature (typically 60°C). This process continues until the LiCl concentration in the LCAR has decreased from its initial value (> 90%) to about 45% at the end of an EVA sortie. The absorbed water is then recovered by heating the LCAR to 100°C, which returns the LCAR to its initial state for use in the next EVA sortie. Figure 2 shows photographs of LCAR and SWME prototypes.

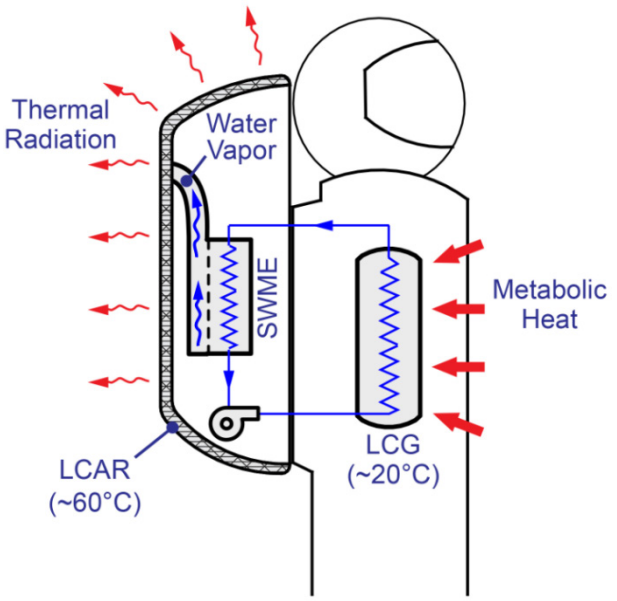

Figure 1. A SEAR system can control temperature inside a spacesuit without venting water.

(a) A 1 ft² Lithium Chloride Absorber-Radiator (LCAR) panel designed to meet flight test requirements

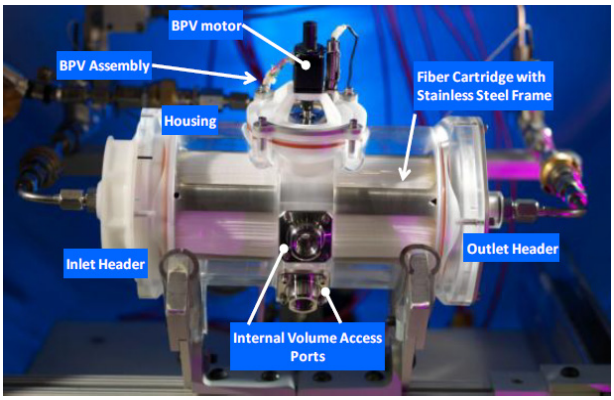

(b) Spacesuit Water Membrane Evaporator (SWME)

Figure 2. LCAR and SWME components of a SEAR system.

This paper describes recent advances in LCAR thermal and structural performance. This work is part of a NASA-sponsored program to develop an LCAR that can be flight tested as part of a subscale SEAR system on an International Space Station (ISS) Extravehicular Mobility Unit (EMU). We have built a series of LCAR panels and measured their performance in thermal vacuum and thermal regeneration tests. The current LCAR design operates at higher heat rejection temperatures than earlier versions, which increases the heat rejection per unit of radiator area.

We have measured performance of the current design across multiple prototypes and multiple absorption/regeneration cycles for a single prototype. The thermal performance of the unit is consistent with expectations based on analysis of thermodynamics of the LiCl/water system. The LiCl absorber bed is housed in a rugged, lightweight titanium shell that has demonstrated the ability to withstand design-basis impacts specified for operation on the ISS without losing LiCl containment and with no observable effects on performance. The burst pressure is greater than 150 psi, giving the prototype a factor of safety greater than 10 relative to the maximum expected operating pressure (MEOP).

II. LCAR Design, Operation, and Testing

An LCAR comprises a thin absorber bed in good thermal contact with a radiating surface. It is used as a regenenerable, swing-bed type system. In absorption mode (~18 torr, ~60°C), the LCAR provides cooling by absorbing water vapor and radiating heat to the environment. In regeneration mode (~9 torr, ~100°C), the LCAR absorbs heat and desorbs water vapor. We have developed test facilities and techniques to measure the performance of LCAR panels in both modes of operation.

A. LCAR Design

The LCAR must be designed to meet challenging requirements for materials compatibility, thermal performance, and durability. Thermal performance requirements are based on the need to reject spacesuit thermal loads using only the area available on a PLSS backpack. The absorber bed must also be securely packaged so that LiCl solution is fully contained under all conditions, including design-basis loads that have been specified for operation on the ISS. Figure 3 shows a solid model of an LCAR prototype with the front (radiating) face removed to reveal the internal absorber bed. Overall dimensions of the flight prototype are approximately 1 ft square by 0.5 in. thick, which have been selected to meet limitations related to the flight test design in which the LCAR is mounted on the EMU's Tile Repair Backpack Frame (TRBF). The absorber bed comprises an array of absorber elements, vapor flow channels, heat conduction pins, and structural pins. The absorber elements are thin plastic sponges that have been fabricated with features that enable good heat and mass transfer performance in the absorber bed. Water vapor enters the bed through the inlet manifold, and residual noncondensible gas (NCG) vents through a capillary. Vapor flow channels are created in the absorber bed using hydrophobic plastic spacers to separate the sponges. Heat conduction pins are thin graphite cylinders that conduct heat through the thickness of the bed, ensuring that the temperature of the bed is close to the temperature of the radiating surface. Structural pins are metal elements that couple the front and back faces of the LCAR and provide strength against impact and pressure loads. Since the LiCl solution corrodes most metals, all the metallic structural components of the LCAR are fabricated from titanium.

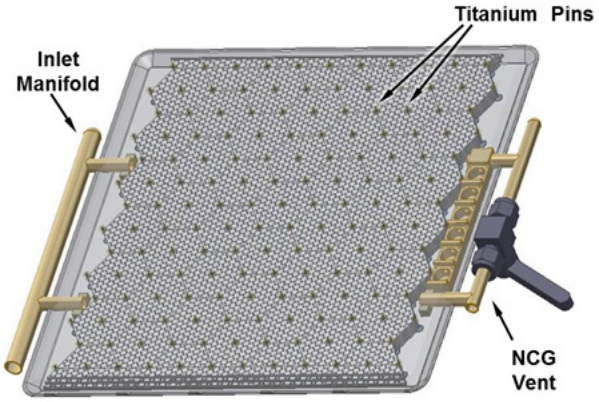

Figure 3. Overall LCAR design. *The radiating surface is removed from this view to show the internal absorber bed.*

Figure 4 is a schematic showing a cross section through the bed, illustrating the general configuration. Table 1 lists the general characteristics of the prototype LCAR. The total dry mass of the of the LCAR is 1,243 g, which comprises 1,043 g of non-absorber (titanium, sponge, graphite, etc.), 190 g of LiCl, and about 8 g of "dead" water that remain after regeneration. The LCAR can be regenerated to a typical concentration of 96%, and reaches concentrations of

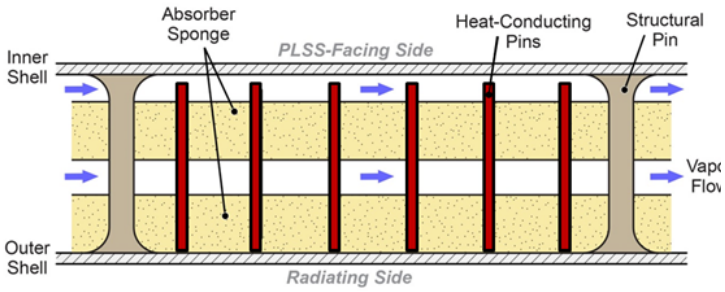

Figure 4. Internal structure of the LCAR absorber bed

roughly 44% at the end of absorption. At the start of absorption, the high-concentration absorbent is a two-phase solid/solid solution of LiCl and lithium monohydrate (Li1). At the end of absorption, the absorbent is a single-phase liquid solution. The concentration swings from very little water to more than half water, and the mass of water absorbed is about 20% more than the mass of LiCl in the bed. This corresponds to a total heat absorption of 579 kJ. During a typical absorption run, the radiating surface temperature will vary from 65°C to 55°C, with an average heat absorption rate of 40 W.

Table 1. General characteristics of flight-like prototype LCAR.

Dimensions	(cm) (in.)	30.5 × 30.5 × 1.3 12 × 12 × 0.5
LiCl mass	(g)	190
Non-LiCl dry mass	(g)	1,045
Dead water mass	(g)	8
Total dry mass	(g)	1,243
Typical concentration swing	(g LiCl / g sol'n)	0.96 to 0.44
LiCl state at start of abs.		Two-phase solid: LiCl+Li1
LiCL state at end of abs.		Single-phase liquid: LiCl/water solution
Water content swing	(g)	236
Heat absorbing capacity	(kJ)	579
Typical duration	(hr)	4.0
Typical absorption rate	(W)	40
Specific cooling power	(W/m²) (W/ft²)	430 40
Specific cooling	(kJ/m²) (kJ/ft²)	6,230 579

B. LCAR Operation

LiCl is a very powerful desiccant. As a result, the LCAR is able to absorb water vapor over a wide range of concentrations and at temperatures roughly 40°C warmer than the SWME. Absorption at this high temperature increases the radiation heat flux and reduces the required surface area of the LCAR. The absorption process is completely reversible, and the water vapor can be recovered by heating the solution to a higher temperature under a rough vacuum.

Figure 5 illustrates the absorption and regeneration cycle. During absorption (Figure 5a), water from the liquid cooling and ventilation garment (LCVG) enters the SWME at a temperature of about 20°C and distributes through an array of hydrophobic, porous hollow fibers. The vapor space in the SWME communicates with the vapor space in the LCAR, which is kept at a very low value (about 18 torr) thanks to the high water affinity of the LiCl/water solution. Since the vapor pressure of the water entering the SWME is higher than the equilibrium vapor pressure over the absorber bed, water evaporates in the SWME. The cooling effect of this evaporation reduces the temperature of the circulating water before it returns to the LCVG. The vapor generated in the SWME flows into the LCAR, where it is absorbed by the solution. Condensation and absorption liberates heat in the absorber elements.

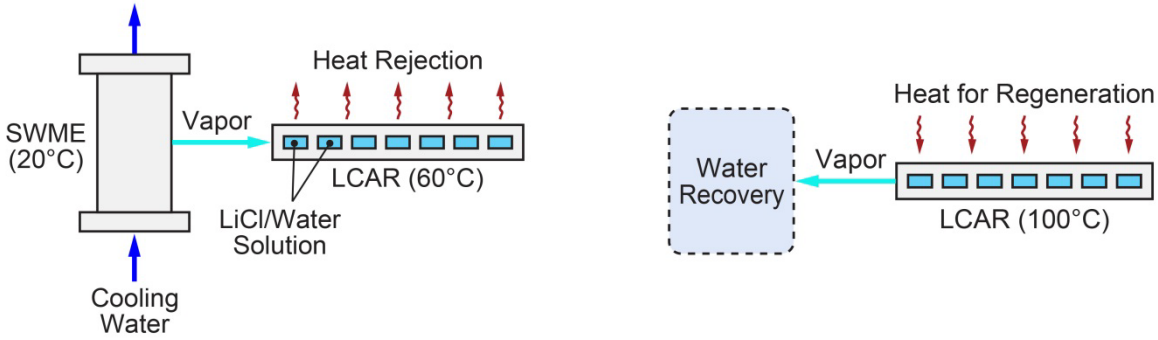

(a) Absorption (b) Regeneration

Figure 5. Absorption and regeneration sequence.

This heat conducts through the bed to the radiating surface of the LCAR, where it radiates to the environment. As this process continues, the concentration in the absorber bed falls, the vapor pressure gradually increases, and the radiating temperature therefore decreases. The LCAR is sized to ensure it can absorb the required amount of water vapor while still operating at a temperature high enough to reject heat to the environment. Figure 5b illustrates regeneration. After an EVA sortie, the LCAR is placed in a regeneration oven inside the spacecraft or habitat module. An oven heats the LCAR while a rough vacuum pump removes water vapor. This process continues until the LCAR temperature reaches a uniform 100°C, at which point nearly all the water has been removed and the LiCl concentration returns to its initial value. The recovered water vapor can be condensed and reused as coolant in the next EVA sortie.

C. LCAR Absorption and Regeneration Testing

A complete LCAR cycle includes both absorption and regeneration (or desorption). Absorption testing takes place in a thermal vacuum test rig that simulates operation in space. Regeneration testing is carried out using a low-temperature oven and vacuum pump, following the same process that would be used in a spacecraft after an EVA sortie.

The absorption test facility comprises a water vapor generator, a vacuum bell jar with an internal test assembly that supports the LCAR panel facing an actively cooled shroud, and a non-condensable gas control subsystem. The schematic in Figure 6 shows the overall test setup. Water vapor is generated in an external loop by a custom capillary evaporator built by Creare. Heat to generate the water vapor is provided by a circulating water loop that is maintained at a constant temperature of roughly 20°C using a temperature-controlled laboratory bath ("Chiller #1" in Figure 6). Platinum resistance thermometers at the inlet and outlet of the evaporator along with a flow meter provide calorimetric data to measure the amount of heat transfer from the circulating loop that produces water vapor. Water vapor flows into the LCAR panel, which operates inside the vacuum bell jar. Non-condensable gas leaves the LCAR through the manifold on the opposite end from the water vapor supply. The gas from the panel flows through a capillary tube, then through a desiccant bed that captures any water vapor lost (for measurement at the end of the test), and finally to a vacuum pump that exhausts to ambient.

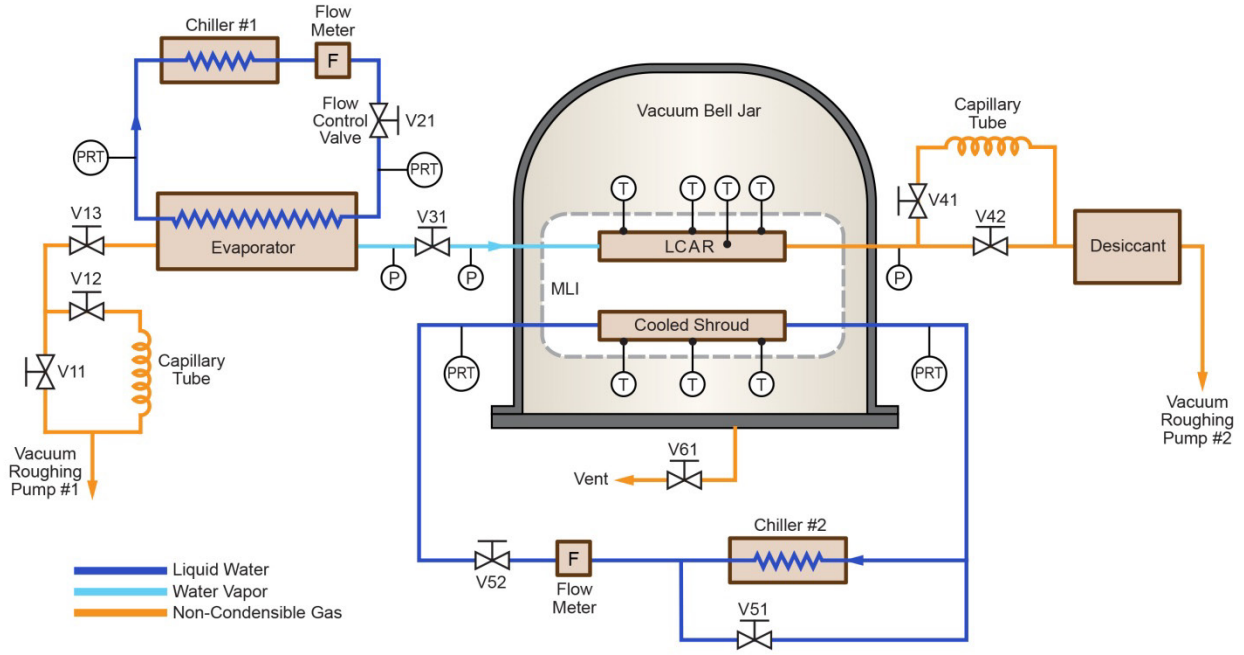

Figure 6. LCAR thermal vacuum test setup.

The photographs in Figure 7 show the vacuum bell jar and the internal frame assembly that supports the LCAR and shroud. The right-hand photo shows the back side of one of the actively cooled shroud panels.

(a) Thermal vacuum chamber

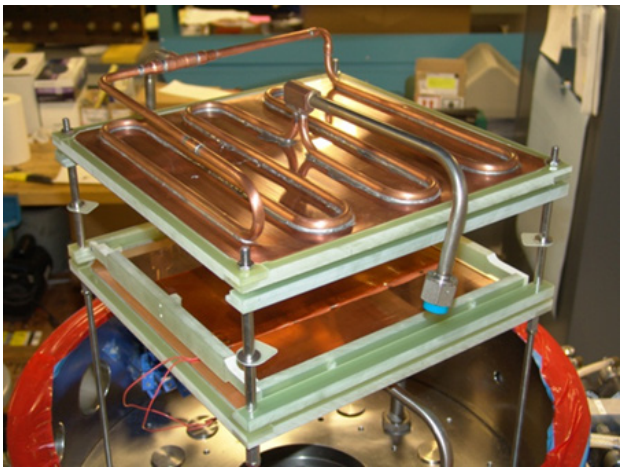

(b) Cooled shroud

Figure 7 Thermal vacuum test facility.

The chamber can accommodate two, 12-in.-square LCAR panels in a back-to-back, stacked configuration, each facing a 14-in.-square cooling shroud, although in the most recent tests we measured the performance of only a single panel. At a separation distance of 0.25 in., this geometry provides a view factor of 0.99 from the radiating side of the LCAR panel to the corresponding shroud, ensuring that we are able to accurately control and measure the heat transfer from the radiator panels. The LCAR panels are supported by small-diameter, stainless steel pins with very low thermal conductance. The heat leak from an LCAR panel operating at 50°C through these pins to the frame running at room temperature is only about 4 W.

The vacuum chamber maintains vacuum levels in the range from 10^{-5} to 10^{-6} torr. At this level of vacuum, the thermal conductivity of the remaining gas in the system is less than 2×10^{-5} W/m-K, which effectively prevents heat conduction from the LCAR to the shroud. For example, for an LCAR temperature of 60°C and a shroud temperature of -25°C, the calculated radiation heat transfer will be roughly 40 W compared to a calculated conduction heat transfer of about 1 mW. Figure 8 illustrates the regeneration test setup.

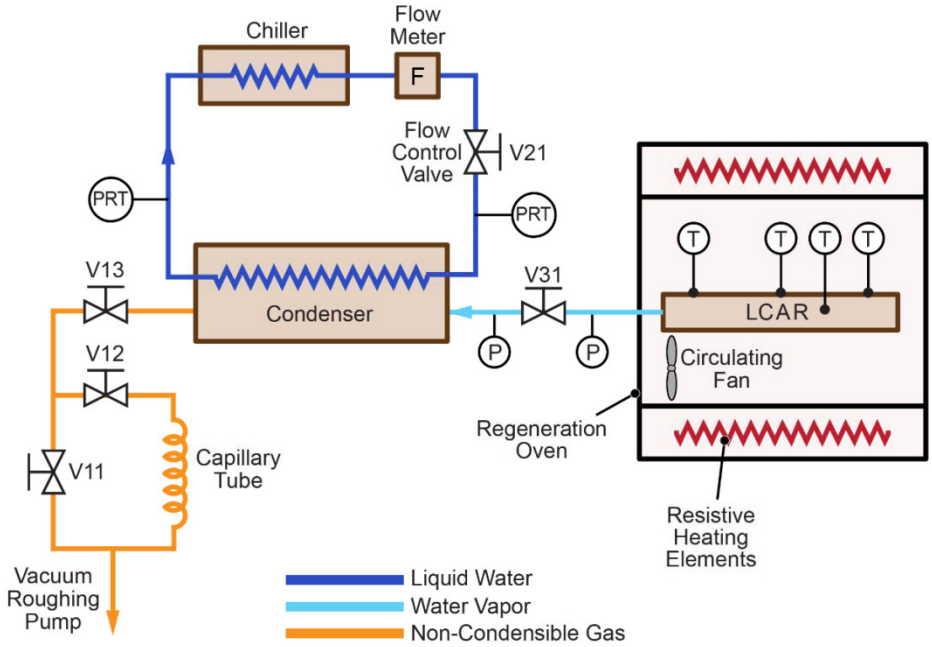

Figure 8. Regeneration test facility.

The regeneration facility has three main elements: the regeneration oven (Figure 9), the condenser subsystem, and the vacuum subsystem. The regeneration oven is an insulated box with internal heating elements and convection

fans to add heat to the LCAR. The rough vacuum pump draws water vapor out of the heated LCAR through the condenser, where nearly all the water vapor is captured on cooled plates that are covered with wicking material. We measure LCAR temperatures during this process. When these temperatures reach a plateau of about 100°C, the regeneration is complete and the concentration has increased to 96%.

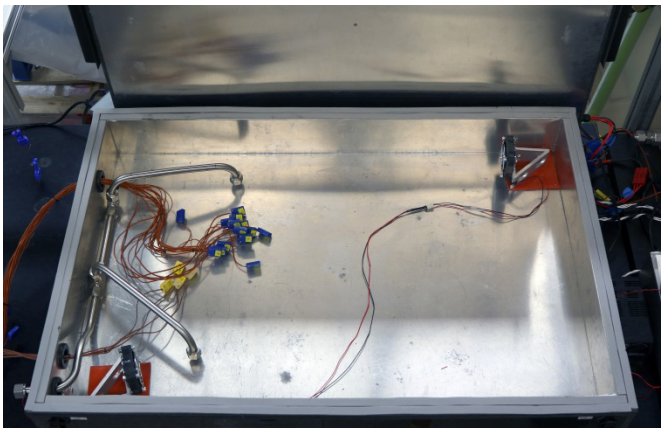

Figure 9. Regeneration oven (LCAR removed).

III. LCAR Absorption

During absorption, the LCAR operates under conditions where the vapor pressure is low enough to absorb water from the evaporator. The flow rate of vapor from the evaporator to the LCAR is determined by the rate of heat rejection. The rate of heat rejection, in turn, is governed by the radiative heat transfer resistance between the LCAR and the heat sink. In most of our testing, these phenomena lead to LCAR operating temperatures that range from 50°C to 70°C for water vapor pressures of 18 torr (corresponding to an evaporator temperature of 20°C).

Figure 10 shows data from a typical absorption run. The left-hand plot shows average temperatures measured inside and on the surfaces of the LCAR, as well as the equivalent evaporator temperature calculated from the vapor pressure at the evaporator exit. The right-hand plot shows the calculated evaporator cooling (based on calorimetry) and the cumulative water absorption based on the calculated cooling. The water mass computed by calorimetry agrees well with the actual change in LCAR mass based on the weight before and after the test. The general decrease in LCAR temperature over time is due to the decreasing concentration as water is absorbed. The step-wise shape of the temperature plot is due to the complex phase behavior of the LiCl/water system (see Section VIII). Likewise, the plot of evaporative cooling power vs. time shows a two-peak characteristic that is common to nearly all absorption runs. We believe that the heat transfer rate is controlled by mass transfer inside the absorber bed, which also depends on how the LiCl solid and liquid phases evolve during the process (Section VIII).

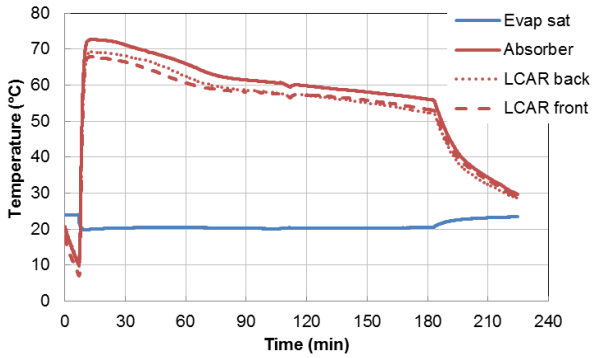

(a) LCAR and simulated SWME temperatures

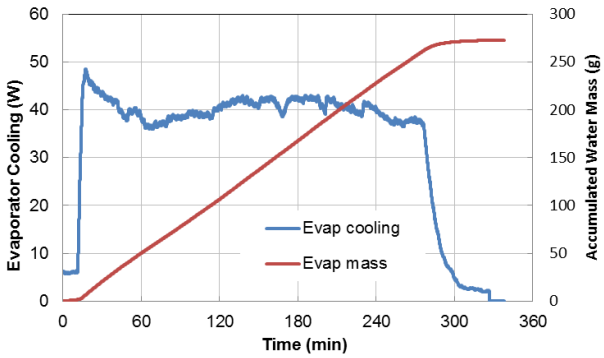

(b) Evaporative cooling and evaporated water mass calculated by calorimetry.

Figure 10. Typical LCAR performance during absorption.

IV. LCAR Regeneration

LCAR temperatures during regeneration also reflect the thermodynamics of the LiCl/water system. Typically, the LCAR will spend most of the time during regeneration at a constant temperature while liquid LiCl/water solution changes phase to become a solid, monohydrate phase. Once all the liquid is gone, the temperature increases to the point where the monohydrate phase can convert to solid LiCl. Figure 11 plots temperatures measured on the LCAR surface during a typical regeneration run. During the long period from 2 hrs and 5 to 6 hrs, the LCAR absorbs heat at constant temperature as the liquid phase depletes. The "left" side of the LCAR (nearest the vacuum ports) dries out more quickly and can increase in temperature before the "right" side. Once the liquid phase has been depleted from the entire bed, the temperature everywhere increases to ~100°C and the process is essentially complete.

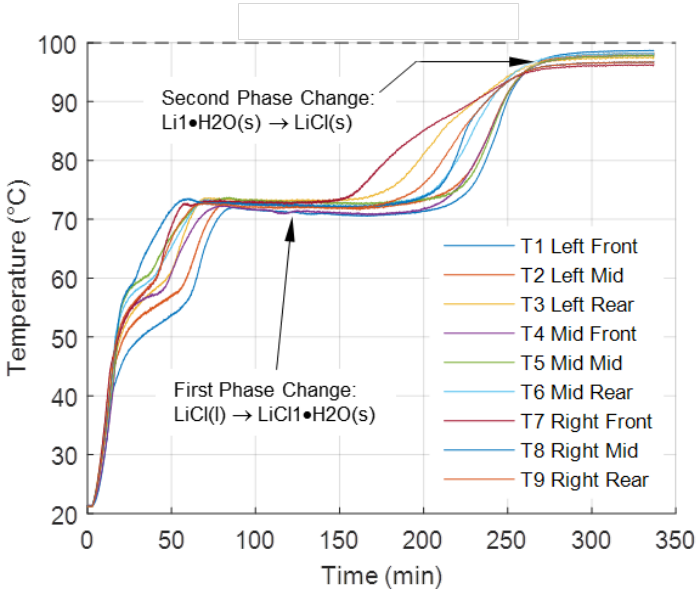

Figure 11. Typical LCAR temperatures during regeneration.

V. Consistency of Performance: Multiple Absorption and Regeneration Cycles of a Single LCAR Prototype

We have run multiple absorption tests of a single LCAR panel to measure consistency of performance between successive runs. Generally, the performance from one absorption run to the next is quite similar. However, we have observed trends that indicate possible migration of LiCl or reduction of vapor flow in the absorber bed that can reduce effective absorption capacity from run to run. Figure 12 shows the performance comparison between four different absorption tests, and Figure 13 shows the mass of water absorbed and regenerated for each run. While the temperature and cooling performance is fairly consistent, the average LCAR temperature decreased by ~1°C for each run from runs 1 to 3. Figure 12a and Figure 12b show the time course of the tests, characterized by a high initial temperature and cooling rate while the solution remains in a solid-solid, LiCl/monohydrate state, shown in Figure 12c and Figure 12d in the concentration change from ~96% to ~70%. As the solution transitions into a solid-liquid state, the temperatures plateau with a slight slope over the concentration range from 70% to 50%, and a change in slope is seen at concentrations below 50% when the solution reaches a dilute liquid state.

In the third test, the LCAR appeared to saturate faster with the temperatures dropping to below 55°C and reaching a lower concentration much earlier than in the previous runs, resulting in a shorter run and less total water absorption. Despite the slightly lower radiator temperature, the measured cooling power remained comparable to previous runs. Some of the temperature difference in run 3 can be attributed to operation at a lower vapor pressure. We used a different evaporator for this run that provided a slightly lower vapor feed pressure (Figure 12e).

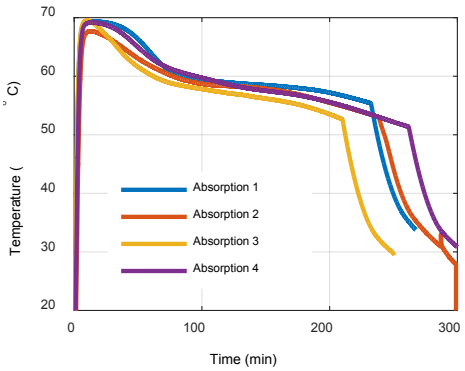

(a) LCAR average temperature vs. time

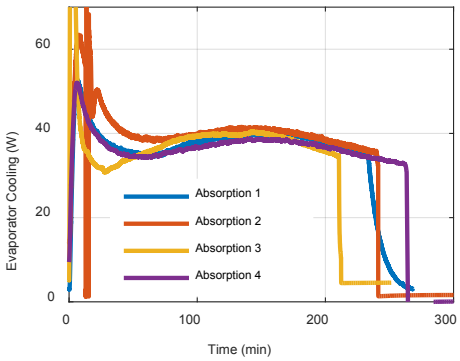

(b) LCAR evaporator cooling vs. time

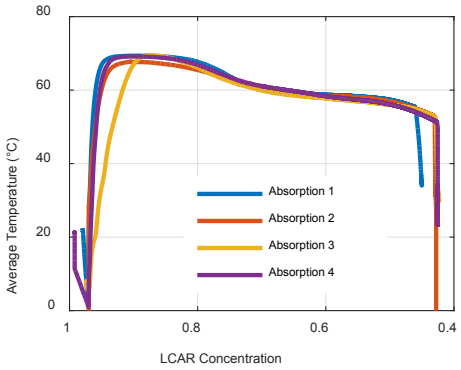

(c) LCAR temperature vs. concentration

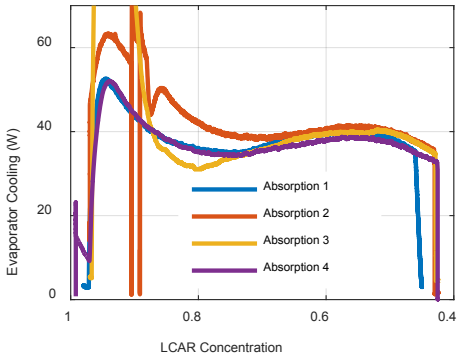

(d) Evaporator cooling vs. concentration

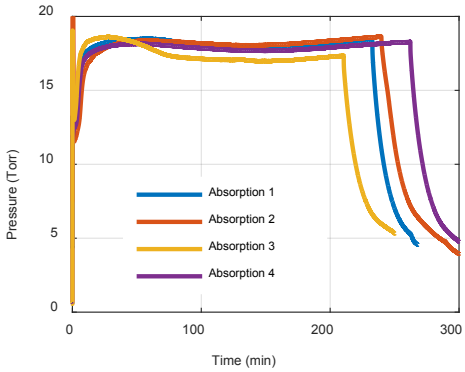

(e) LCAR vapor inlet pressure

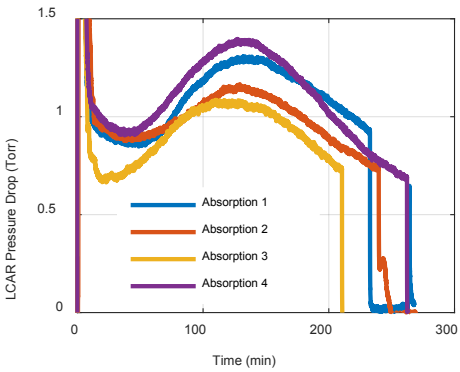

(f) Pressure drop across LCAR

Figure 12. Comparison of successive absorption tests on a single LCAR.

Figure 13 shows the change in LCAR mass after each absorption or regeneration run, which is equal to the change in water mass. Note that each regeneration succeeds in removing the same amount of water that is absorbed in the prior absorption run. However, the amount of water absorbed can vary noticeably from run to run (particularly for run 3) depending on test and absorber conditions. We measure the concentration in the LCAR at the end of each run by closing off the vapor feed and recording the pressure-temperature (P-T) curve as the LCAR returns to ambient temperature. These data are compared to curves of the vapor pressure over LiCl solution at varying concentrations. The concentration measurement after run 3, shown in Figure 14 indicates a solution concentration of

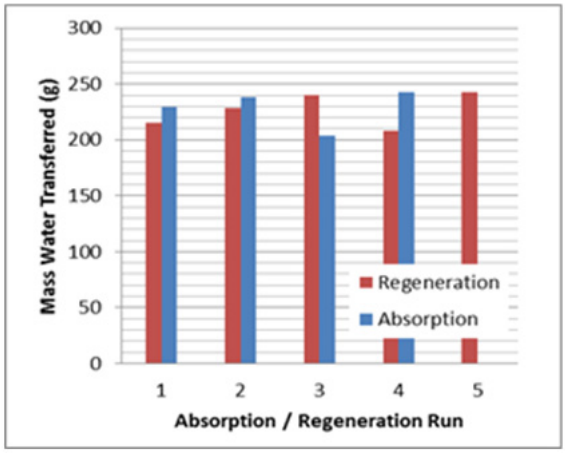

Figure 13. Water mass transferred to and from the LCAR during successive absorption and regeneration cycles.

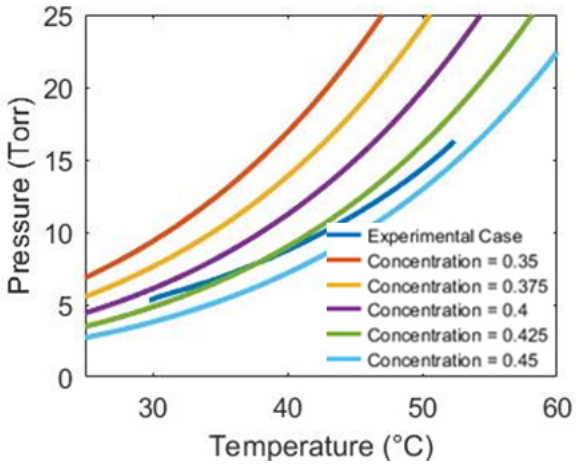

Figure 14. Post-absorption concentration measurement for run 3.

~42.5%, whereas the final concentration based on the quantity of water absorbed and the total estimated salt content of the LCAR should be 46.6%. This discrepancy may be due to (1) the solution in the LCAR not reaching full equilibrium at the end of the test, and a layer of more dilute liquid solution at the solution/vapor interface controls the vapor pressure measured during the cooldown; and/or (2) a section of the LCAR receiving less vapor flow, which removes some of the salt from participating during absorption. If some of the salt were isolated from contact with water vapor, then the accessible salt becomes a more dilute solution. As the concentration falls, the enthalpy of dilution drops, which reduces the radiator temperature for the same rate of water absorption/evaporator cooling.

The concentration measurements based on the pressure/temperature behavior of the LCAR panels provide bounds of the final dilute state of the radiator, but this approach has some uncertainty associated with it. As can be seen in Figure 14, the experimental data is closest to the 42.5% curve, but the slopes do not line up perfectly, and a range of ±2.5% is possible depending on which temperature range is inspected. However, very small changes in final concentration result in larger uncertainty of the estimation of active salt mass. If the LCAR solution has not fully equilibrated during the P-T measurement, a lower quantity of salt will be assumed than may actually be participating. Using the component weights of the LCAR during construction and the tracked water masses over each absorption and regeneration run, we determined that this LCAR has a salt loading of ~190 g. If all 190 g participate in an absorption, the final concentration of each run can be determined based on the quantity of water absorbed. Table 2 compares the ending concentrations that are predicted for each run using this estimation method and the P-T cooldown measurements and shows the uncertainty in active salt that results from a ±2.5% uncertainty in the P-T concentration measurement. Aside from the third absorption run, the two approaches to determine the final concentration match fairly well. Flowing vapor in the reverse direction for run four seems to have helped return full salt activity to the LCAR.

Table 2. Comparison of ending concentration estimations for successive absorption runs.

	Starting Concentration	Ending Concentration Based on Water Mass	Measured P-T Curve Ending Concentration	Active Salt Measured from P-T Concentration (g)
Fabrication	–	45.2%	--	189.5
Absorption 1	92.8%	43.7%	45.0%	176.5 ± 12.2
Absorption 2	92.6%	42.8%	43.5%	183.4 ±10.2
Absorption 3	93.5%	46.6%	42.5%	157.3 ± 11.9
Absorption 4	95.6%	43.0%	42.5%	189.5 ± 11.4
Final Regeneration	95.8%			

Figure 12f shows that the pressure drop across the LCAR from the vapor inlet to the non-condensable gas outlet (before the capillary restriction) was initially higher during run 4 than in previous runs and decreased rapidly toward the end of the test, corresponding with the dilute, liquid phase. This could be caused by solid salt building up in the vapor flow channels, increasing vapor flow resistance until absorbing enough water to dissolve the solid phase and reabsorb into the sponge elements. Further tests will help us determine if there are significant changes taking place within the LCAR that are causing continued performance degradation, or if these results represent a normal variability in operation.

VI. Absorption and Regeneration Cycles for Multiple LCAR Prototypes

We have compared absorption performance of different LCARs and have found similar performance, indicating that the fabrication methods used to produce the LCARs have achieved good consistency. To date, we have tested three different LCARs. Figure 15 compares all absorption runs from each LCAR tested. LCAR 2 has a different absorber bed design than LCAR 3 and LCAR 5, which allows it to achieve a higher salt loading. Because of this, LCAR 2 slightly outperformed the configuration used in LCARs 3 and 5. LCAR 2 also has more vapor-flow layers as part of its absorber configuration, which yielded a lower pressure drop across the absorber. However, the LCAR 2 configuration is significantly thicker and requires compression to fit within the titanium shell, complicating the fabrication and welding and increasing the risk of developing leaks at the titanium pin weld sites. LCAR 5 was tested using a hollow fiber evaporator which has less thermal mass than the evaporator used for the previous tests, resulting in a faster response and higher measured values of the initial cooling rates. All the runs show consistent

trends and exhibit similar cooling performance, though LCAR 5 has a slightly lower cooling performance (~5% lower than LCAR 3).

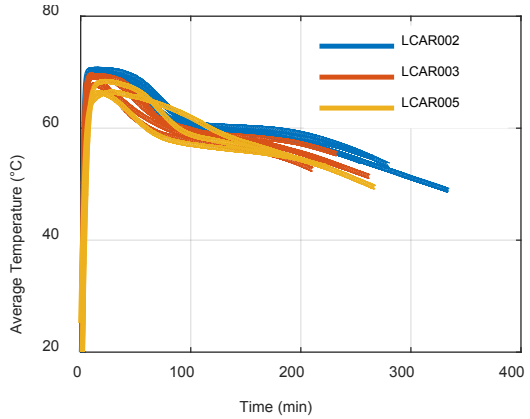

(a) LCAR Average Temperature During Absorption

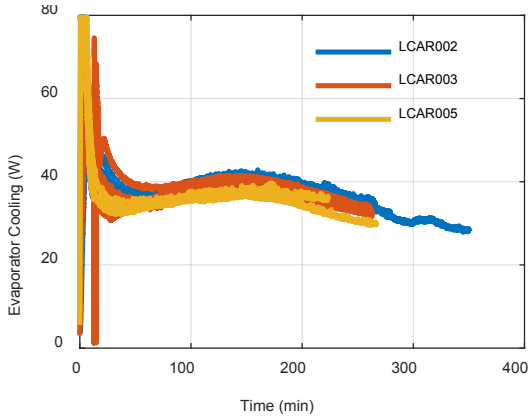

(b) LCAR Evaporator Cooling During Absorption

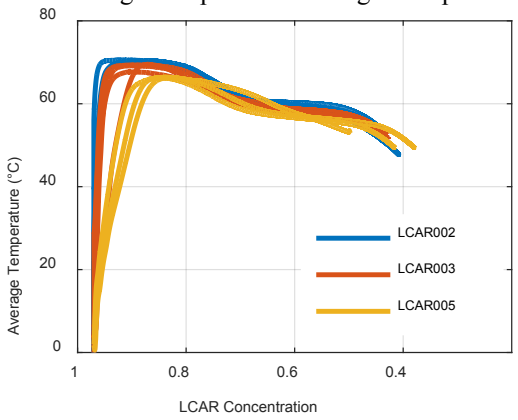

(c) LCAR Average Temperature vs Concentration

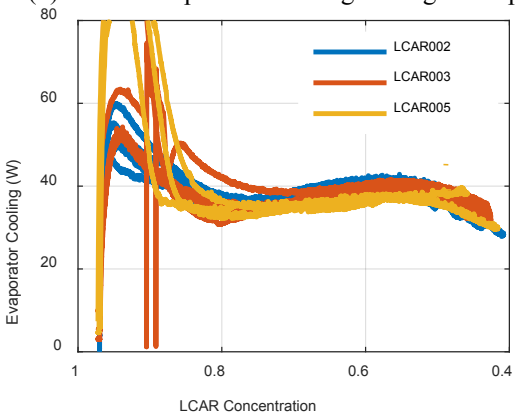

(d) LCAR Evaporator Cooling vs Concentration

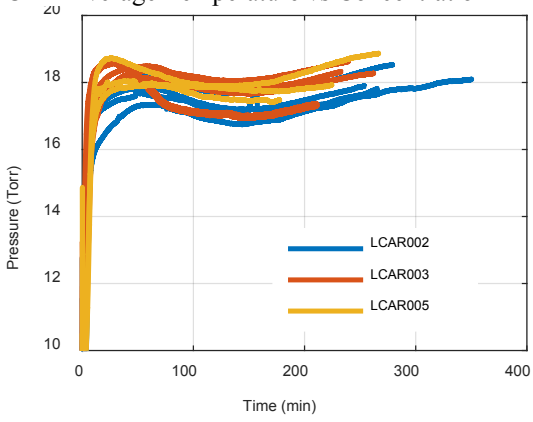

(e) LCAR Vapor Inlet Pressure During Absorption

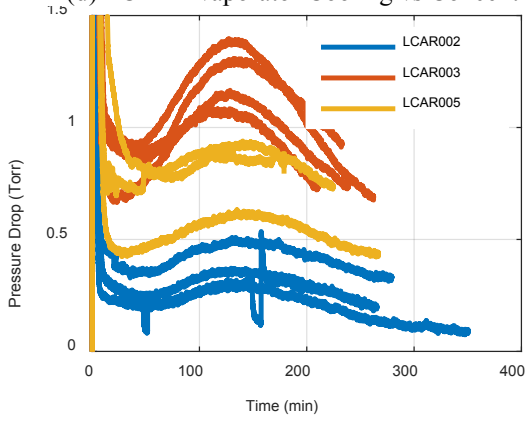

(f) Pressure Drop Across LCAR

Figure 15. Comparison of absorption tests for different LCARs.

VII. LCAR Structural Performance

The LCAR's absorber bed is housed inside a rugged titanium shell. Prior papers have documented that the shell structure can withstand design-basis impacts that are specified for operation on the ISS without losing containment of LiCl. These early tests used small (4-in.-diameter) structural samples. Since then, we have simulated impacts on complete (1 ft²) LCAR panels and shown that the simulated impact had no observable effect on LiCl containment or

on the LCAR's thermal performance. We have also demonstrated that the titanium shell has a very high-pressure retention capability, well beyond margins that are required for flight operation.

Impact Test. To demonstrate the impact resistance of the LCAR panel structure, we placed a functional LCAR between a flat plate and a 2 in. steel ball in a hydraulic press. The LCAR was oriented with the steel ball contacting the LCAR's radiating face. The rigid flat plate included a high-durometer rubber sheet between the plate and LCAR designed to protect the surface-mounted thermocouples used during performance testing. The rubber sheet deflected no more than 7 mil during the test and contributed no more than 3% of the total strain energy absorbed. To simulate the impact, we gradually increased the force of the ball against the LCAR until the target impact energy was reached. We measured the displacement using a dial indicator on top of the rig and then measured the force with a transducer located beneath the flat plate. We calculated the work done by integrating the force as a function of displacement. We halted loading once the integrated work reached 154 in.-lb_f or 17.4 J, the impact energy specified for the EMU. The test setup for the full-size LCAR is shown in Figure 16.

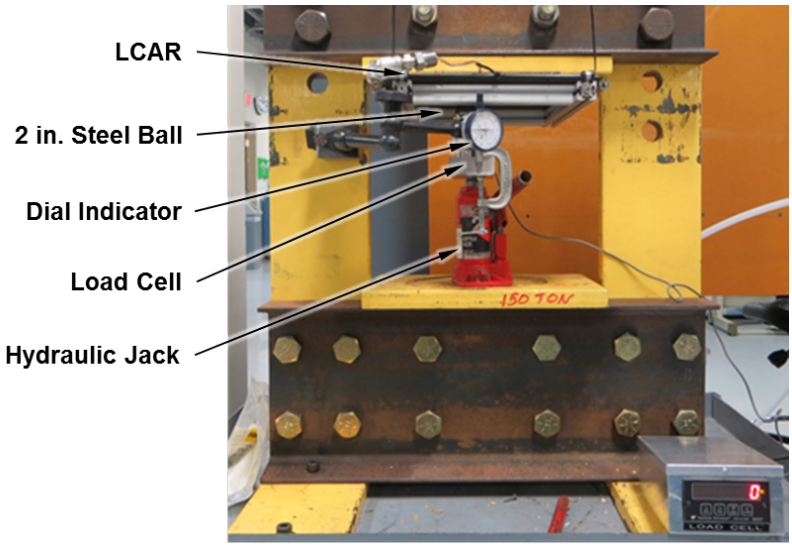

Figure 16. Full-scale LCAR impact test setup.

Figure 17 shows the LCAR following the impact tests. Figure 18 shows the measured force and deflection data, along with the calculated energy absorbed during the sponge region impact test. The sample reached the required 154 in.-lb_f with a deflection of about 0.32 in. After the impact test, we leak-checked the panel and found that it was still leak tight. We flooded the LCAR with helium and used a mass spectrometer to check for leaks in the LCAR. After none could be detected, we checked the leak-up rate on the LCAR. We found no discernable difference in the LCAR leak-up rate, suggesting the impact had no negative effect on the LCAR's hermeticity.

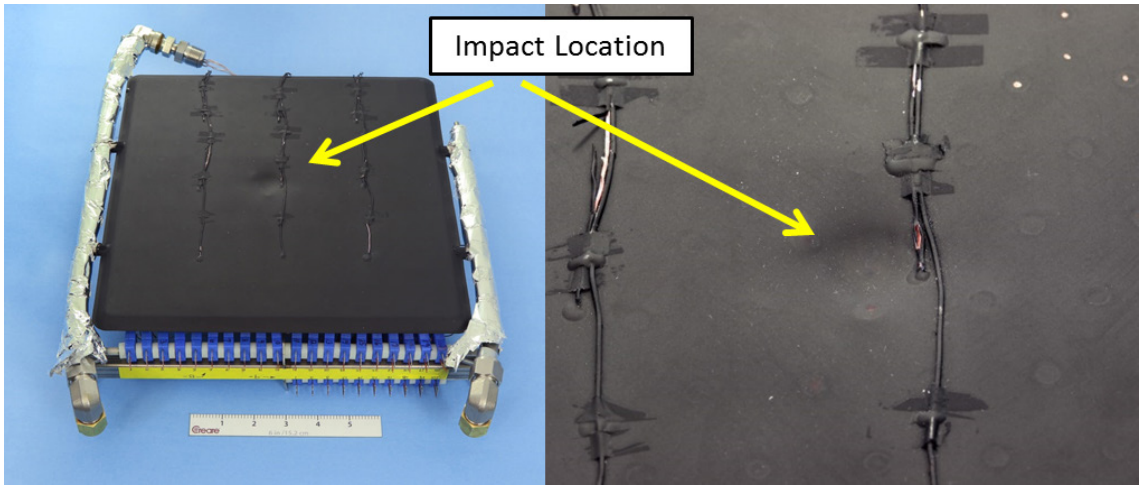

Figure 17. LCAR radiating surface after impact test.

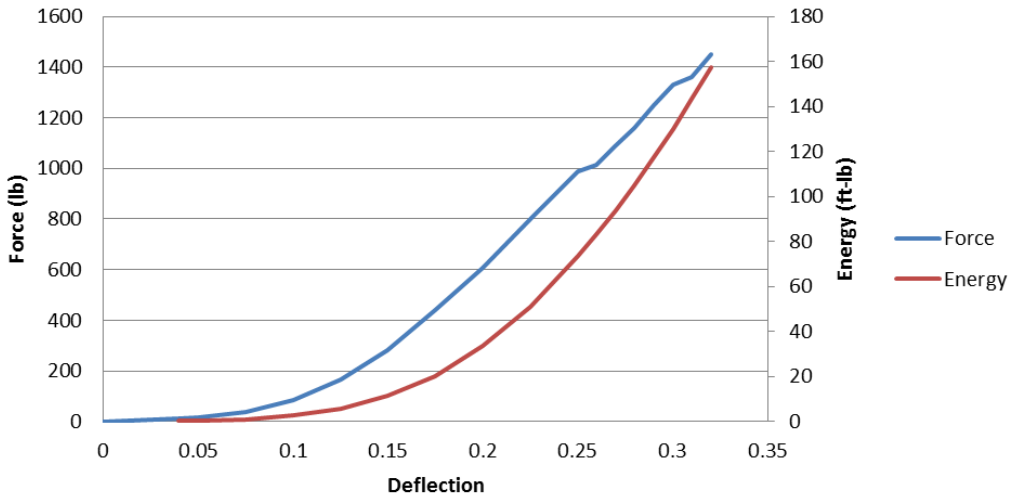

Figure 18. Force/deformation/energy absorption data from impact test.

After the impact test, we ran an additional absorption test of the LCAR to measure performance and see if we could detect any degradation from the impact. The post-impact and pre-impact absorption tests were performed under similar test conditions, and we could observe no significant degradation in the LCAR's performance. We absorbed 272 g of water into the LCAR over the 280-minute test, averaging 40 W of heat absorption. The pre-impact baseline absorption test absorbed 328 g of water into the LCAR over the 350-minute test, averaging 38 W of heat absorption. Figure 19 compares the sponge temperatures for the pre-impact and post-impact absorption tests. Figure 20 compares the heat loads absorbed by the LCAR for the pre-impact and post-impact absorption tests. The fluctuations in the pre-impact test heat load signal is due to poor temperature stability of the chiller used in the water evaporation flow loop. The post-impact test employed chiller with much greater temperature stability.

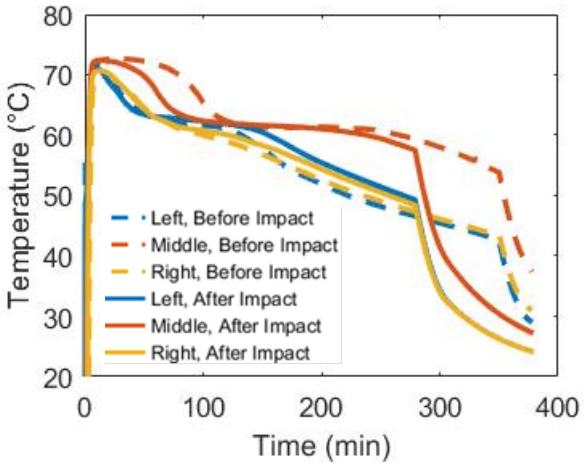

Figure 19. Comparison of sponge temperatures during absorption tests before impact (dashed lines) and after impact (solid lines). *Sponge temperatures are color coded by location in the LCAR.*

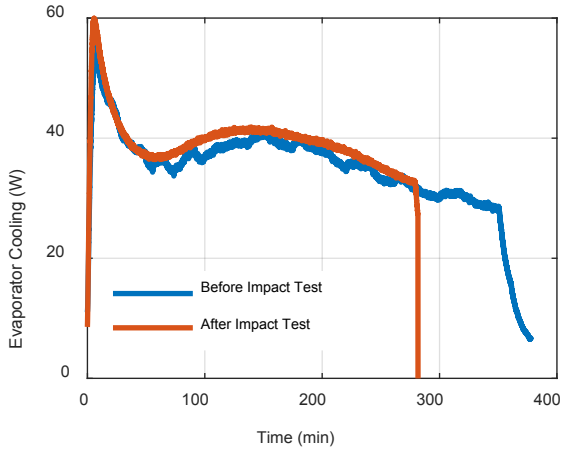

Figure 20. Comparison of heat loads before and after impact testing. *A less accurate chiller was used to control the evaporator for the pre-impact test, resulting in a noisier signal.*

From these results, we concluded that the impact event had no significant effect on the panel's thermal performance. Though the LCAR's internal structure was compacted at the point of impact, the absorber bed is built with enough redundancy for vapor flow and internal heat conduction that the effects of a single impact were not observable.

Internal Pressure Test. We measured the response of a full-scale LCAR panel to high positive internal pressure. The LCAR is never expected to be pressurized beyond 14.7 psig during operation. To assess the LCAR's safety factor for overpressure, we set up to measure the LCAR's burst pressure. The test system is shown in

Figure 21. A regenerated (dry) LCAR panel was placed in a containment vessel. The inlet of the LCAR was connected to a regulated pressurized air source, and the outlet was capped. We increased the LCAR internal pressure in increments of 10 psi.

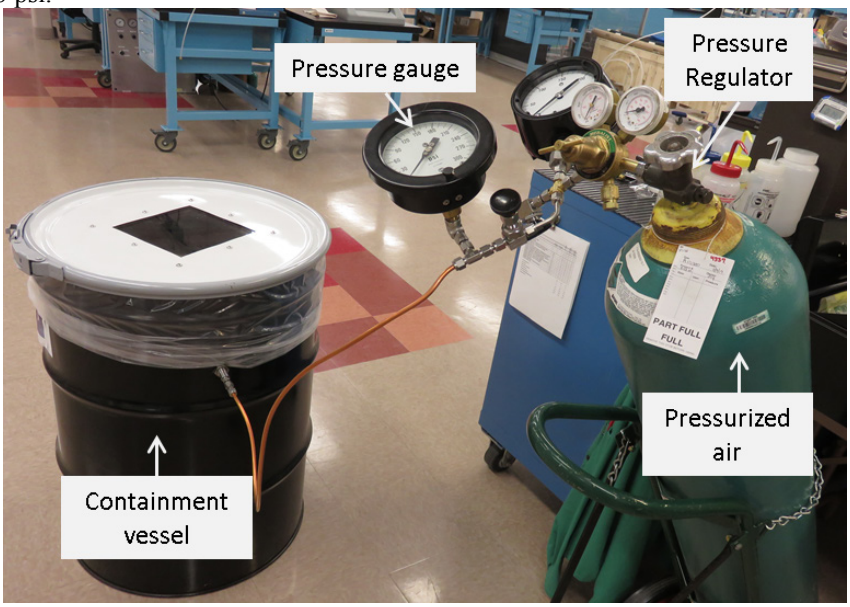

Figure 21. Pressure test setup.

Figure 22 shows comparison photographs of the unpressurized LCAR and the same LCAR when pressurized to 150 psig. The panel exhibited minor elastic deformation of the surface at 150 psig. After the LCAR internal pressure was restored to 0 psig, the material sprung back with no evidence of deformation. Although we terminated the testing at 150 psi and were not able to measure the burst pressure, we concluded that failure due to overpressure is extremely unlikely.

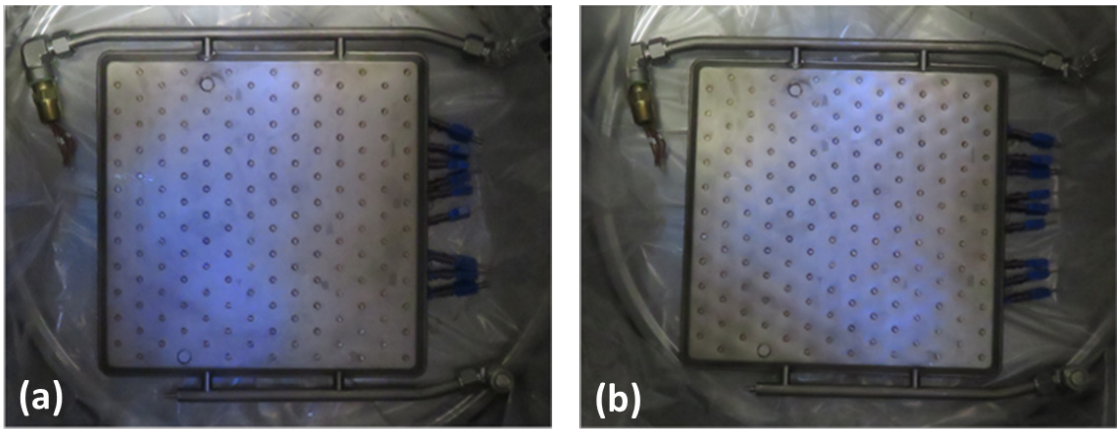

Figure 22. (a) Unpressurized LCAR. (b) LCAR pressurized to 150 psi. *All deformation was elastic, and the surface returned to normal after the test.*

VIII. SEAR Coolant Assessment and Preliminary Testing

UTAS undertook to identify and demonstrate a formulation and process for a water-based coolant that would be compatible with the SEAR system. This coolant would be utilized for a spacesuit application of an SWME cooling device. Key characteristics such as stability (chemical and microbiological) over extended periods of time were key drivers to this selection process. Additives, if used in such a coolant, would need to be non-volatile, or if volatile, should not be detrimental to the performance of the LCAR.

Candidate coolants are listed in Table 3, along with their advantages and disadvantages. Our assessment is that elemental iodine coupled with a periodic scrubbing process with an ion exchange resin/organic adsorbent is the optimal approach to maintain the quality and stability of the coolant to be used for the SEAR LCAR application. This approach uses the Airlock Cooling Loop Recovery (ALCLR) hardware that is already used on the space station, and is listed in the bottom row of Table 3. The ALCR approach takes into account lessons learned from the Advanced Suit (PLSS 2.0) ground testing as well as the many years of successfully using the ALCLR hardware and process with the ISS EMU. The other considered approaches were less attractive due to a number of reasons, including prior use with observed shortfalls (elemental silver), limited benefits (strategically located filters), and lack of technical maturity (silver coupled with an organic compound to enhance stability).

Table 3. Potential coolants and biocide approaches for a SEAR system.

Biocide Option	Pros	Cons
Iodine/Silver as Currently Used (no scrub)	• System use precedent set for iodine • EMU compatibility for technical demonstration on ISS	• System use precedent not set for silver (corrosion risks) • Complexity, crew time hit • Short life for both biocides (no residual) • No scrub to remove contaminants with silver
Strategically Located Filter(s)	Reasonably mature technology for aircraft-potable system target	• Point control, not system control • Need to couple with scrub
Wetted Material Surface Treatments	• Simplicity once the hardware is manufactured • No crew time	• Further development needed • Adds complexity to hardware manufacture • No scrub to remove contaminants
Iodine Complexed With an Organic	• Potential for long-term life • Potential for limited matls. risk • Low crew time	• Unproven • New biocide, need to couple with scrub • Need means to introduce to the system

		• Loss in vacuum (evaluating a remedy)
Silver Complexed with an Organic	• Potential for long-term life • Potential for limited matls. Risk: Lower crew time	• Unproven • New biocide to have accepted, need to couple with scrub • Need means to introduce to the system • Low pH (evaluating a remedy)
ALCLR Tailored to the SEAR Application: • Ion/organic contaminant periodic scrub • Iodine disinfectant	• Based on precedent, but simpler • Acceptance of near-term ISS tech demo with an EMU or other appl. » Reduced crew time » Coupled with scrub » Sized for the need	• Needs further development for SEAR/SWME appl. • Iodine transfer challenges (remove after disinfection if detrimental to LiCl functionality)

UTAS ran experiments to observe and measure the expected fate of iodine in a SEAR LCAR application. Testing with a commercial membrane bundle and 4 ppm iodine in water solution clearly demonstrated that iodine will evaporate through a SWME membrane and will transfer via the vapor route to the LiCl in an LCAR. In a worst-case scenario, a total of 400 ppm of iodine in LiCl would accumulate during a 50-EVA use scenario, assuming 100% of the iodine used evaporated and remained bound to the LCAR LiCl through use and regeneration cycling. At the time of this writing, testing was underway to determine the amount that could be expected to transfer and remain permanently bound to LiCl, but it is expected to be far less than 400 ppm.

Additionally, at the time of this writing, testing was under way to determine if trace amounts of iodine bound to LiCl would adversely impact the amount and rate of LiCl absorption of water. Given the lack of literature information on the impact of iodine on LiCl moisture absorption and the trace amounts of iodine expected, no detrimental effects are anticipated. Even at the maximum possible concentration of 400 ppm (0.04%), the amount of iodine in the LCAR will be orders of magnitude less than the amount of chlorine (the minimum LiCl concentration is about 45%), so we expect very little effect on LCAR performance.

A process similar to that used for the ISS EMU maintenance of cooling water is recommended for the SEAR LCAR application. After each EVA, the spacesuit would be returned to the manned facility, and the LCAR would undergo heat desorption for water recovery. In parallel, the spacesuit cooling loop would undergo closed-loop scrubbing with an ALCLR-like ion exchange resin/organic adsorbent treatment bed. Thereafter, a bed packed with iodine resin would be interfaced with the spacesuit cooling loop for a closed loop disinfection cycle with iodine. If trace amounts of iodine are found to not be detrimental to the functionality of LiCl, then the process would end here. If trace iodine is found to be detrimental to the functionality of LiCl, then the iodine would then be scrubbed out of the spacesuit cooling loop with the ALCLR-like ion exchange resin/organic adsorbent bed after an appropriate iodine/disinfection dwell time. If the spacesuits were to remain idle for significant periods of time (> 90 days), the cooling loops would undergo additional scrubbing/disinfection cycles as is the case with the current ISS EMU.

IX. Discussion

The general characteristics of LCAR behavior during absorption and regeneration can be explained based on the complex phase behavior of the LiCl/water system. The observed degradation in LCAR performance over the course of several absorption/regeneration cycles is probably due to the flow of liquid solution in the bed and buildup of salt in specific regions. We believe this can be prevented in future prototypes by incorporating improvements in the bed design to stabilize the liquid location.

Thermodynamics of LiCl/Water Solutions. The LiCl/water system has a complex phase behavior that affects operation of the LCAR. After regeneration, an LCAR typically begins an absorption run in a solid/solid two-phase state, transitions through a two-phase liquid/solid state, and finishes as single-phase liquid. These different states of the system have different vapor pressure characteristics depending on the number of phases. Two-phase regions have a single vapor pressure that increases with temperature but is independent of concentration, while the single-phase region has a vapor pressure that depends on both the temperature and concentration. Since the LCAR typically operates at a single vapor pressure that is set by the evaporator conditions, these vapor pressure/phase relations control the operating temperatures for the LCAR.

Figure 23 shows the phase diagram for the LiCl + water system, showing multiple regions that can be either single- or two-phase containing liquid and/or solid phases. The x-axis of the plot is the LiCl concentration (g LiCl/g of solution) and the y-axis is the temperature. The region labelled “LCAR” shows typical conditions during

absorption. At low concentrations and higher temperatures, the solution exists as a single-phase liquid. However, solid phases begin to precipitate at higher concentrations. At typical LCAR temperatures, a solid lithium monohydrate (Li1) phase appears at concentrations above ~50%. As the concentration increases above 50%, the fraction of liquid decreases while the fraction of Li1 increases, until the system is completely solid at a concentration of about 70%. At concentrations greater than 70%, a solid LiCl phase begins to appear. The region between 70% and 100% is characterized by a two-phase solid/solid region.

Figure 24 shows the vapor pressure of LiCl + water over a range of concentrations and temperatures that span typical LCAR operating conditions. In this plot, the amount of LiCl present is represented as the mass ratio or water loading, W, which is the mass of water in the system per unit mass of dry LiCl. A water loading of 0 corresponds to a LiCl concentration of 100%. The plot shows vapor pressure behavior at temperatures ranging from 30°C to 90°C, and also indicates the three different phase regions (liquid, liquid + Li1, and Li1 + LiCL) that are relevant to LCAR operation. The vapor pressure is independent of water loading in the two-phase regions, but increases with water loading in the single-phase liquid region. The data shown in Figure 24 have enabled us to construct an interpolation function to calculate the vapor pressure over LiCl + H_2O across the entire range relevant for LCAR operation. Figure 25 plots the data and curve fits for the single-phase liquid region, and Figure 26 plots the vapor pressure as a function of temperature in the two solid/solid regions. The solid lines that are shown in Figure 24 show the vapor pressures calculated by the interpolation function, which line up well with the data across the entire range.

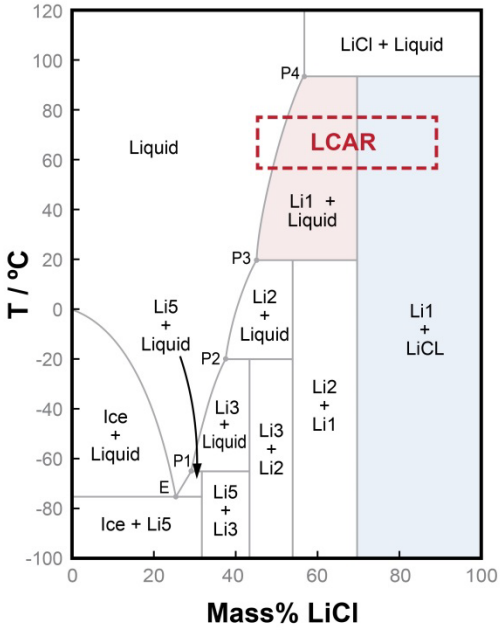

Figure 23. Phase diagram for the Licl/water system.[4]

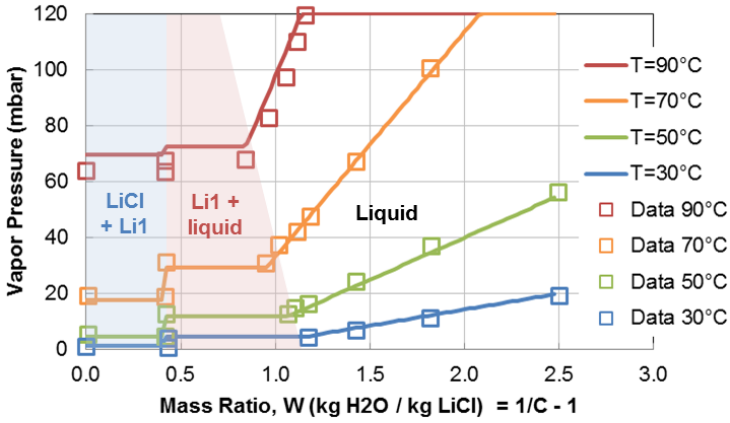

Figure 24. Vapor pressure characteristics of LiCl/water solution.[5]

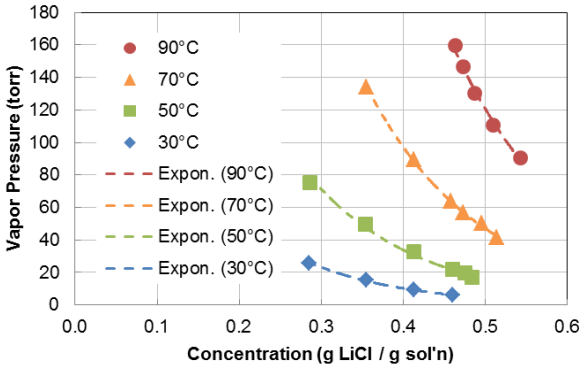

Figure 25. Vapor pressure vs. temperature and concentration over single-phase liquid solution.

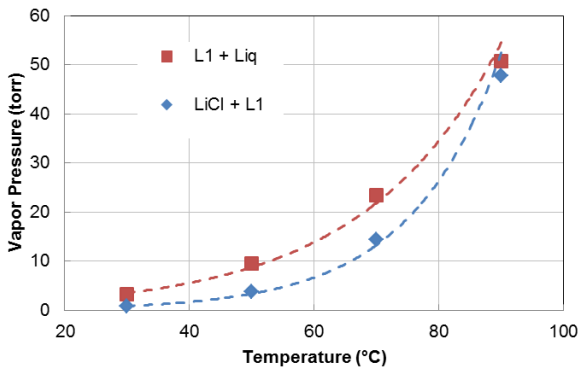

Figure 26. Vapor pressure vs. temperature in two-phase regions.

Implications for LCAR Operation. The vapor pressure properties of the LiCl and water in the desiccant bed control the LCAR temperature and lead to a characteristic two-step behavior that we observe in every absorption run. Figure 27 shows the vapor pressures in the evaporator and LCAR during a typical absorption run, showing that the process occurs at a constant water vapor pressure. Figure 28 plots temperature and vapor pressure data for LiCl + H_2O as a function of concentration and relative to the vapor pressure (17 torr) in a 19.5°C evaporator. The process begins at the right of the chart at the point labeled "1." The starting concentration is high (typically > 95%) and the LiCl solution is in the two-phase solid/solid LiCl+Li1 state. As the bed absorbs water and the LiCl concentration decreases, the vapor pressure remains constant and therefore the temperature remains constant as well. The temperature in the LICl+Li1 region that corresponds to 17 torr is 74°C, and the equilibrium temperature will remain at this level until the bed undergoes a phase change to Li1+Liquid at a concentration of about 70% (point "2" in Figure 28) The new equilibrium temperature for this phase is 65°C, and this temperature will persist until the concentration is low enough for single-phase liquid to appear (at point "3"). Once the bed contains single-phase liquid, the temperature falls rapidly with decreasing concentration, typically ending in the 50°C to 60°C range (point "4").

Since the conditions in the desiccant bed are not entirely uniform, this behavior is observable mainly in an approximate way. Figure 29 shows temperature measurements during a typical absorption run. Temperature data come from 27 thermocouples mounted in 3×3 arrays on the LCAR radiating surface, on the LCAR's non-radiating surface, and inside the LCAR embedded in the desiccant bed. The central thermocouple of each array is located at the center of the LCAR, and the remaining eight are spaced about 3 in. apart in a square array. The data in Figure 29 are averaged over each of the arrays corresponding to the radiating side ("front"), non-radiating side ("rear"), and inside the desiccant bed ("mid"). Since the mid thermocouples are in the desiccant bed, they should correspond most closely to the temperatures indicated by Figure 28.

Figure 29 also indicates the same points 1 to 4 that are shown in Figure 28. The points are placed on the plot by calculating the average bed concentration based on water absorbed (which, in turn, is inferred from calorimetry on the evaporator). The periods 1 to 2 and 2 to 3 correspond to two-phase behavior of the LiCl/water system, while the period 3-4 corresponds to single-phase liquid solution. The changes in slope and temperature are in rough agreement with expectations based on the thermodynamic properties of LiCl+H_2O.

Evaporating Power. Figure 30 plots the heat load during the same absorption run shown in Figure 29. Nearly all absorption runs show this basic cooling behavior: There is a large initial peak in cooling power when water vapor enters the LCAR, followed by a much more gradual increase and decrease in cooling power. The initial peak occurs when the vapor/solution interface in the desiccant bed quickly reaches equilibrium with the evaporator. However, the water absorbed at the interface can penetrate the desiccant bed only by diffusion through solid phases, which is relatively slow. As a result, the cooling power decreases rapidly following the initial peak. Liquid begins to form at point 2 and enhances the rate of water transfer from the vapor/solution interface. As a result, the cooling power rises gradually as the mass transfer resistance falls. As more water is absorbed, the thickness of the liquid layer increases and adds additional mass transfer resistance. Eventually, the cooling rate decreases gradually as the mass transfer resistance of the liquid layer grows.

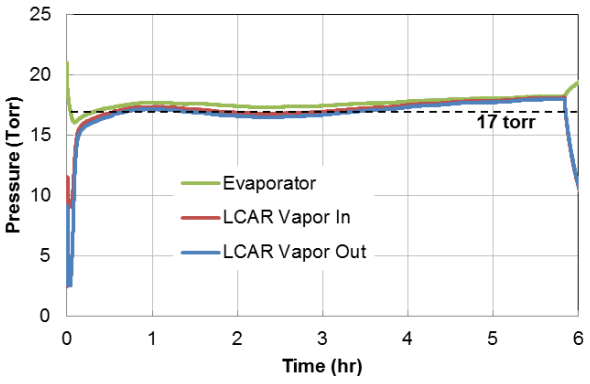

Figure 27. Vapor pressure in an LCAR during water vapor absorption.

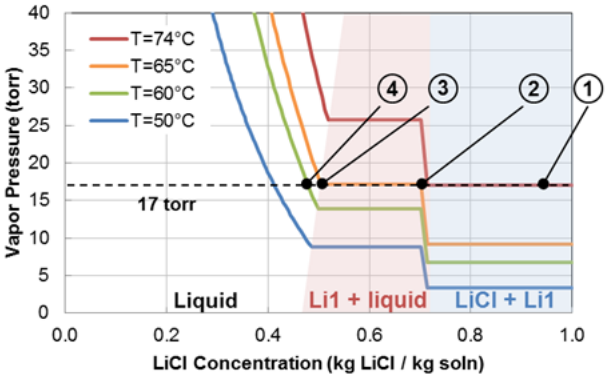

Figure 28. Phase, temperature, and vapor pressure behavior of an LCAR during absorption.

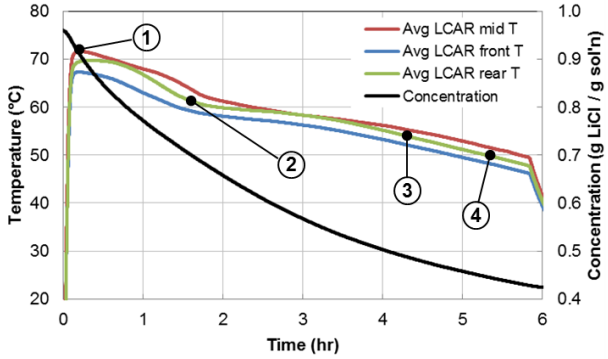

Figure 29. Average LCAR temperatures and LiCl concentration during absorption.

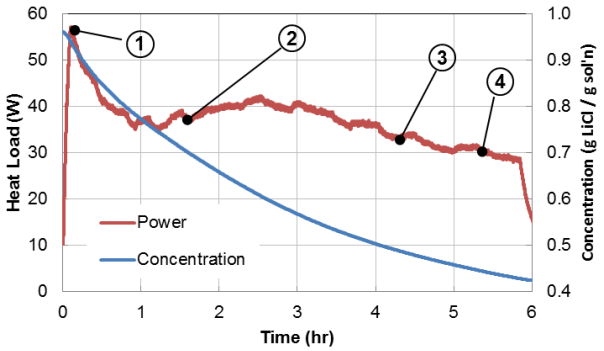

Figure 30. Evaporator cooling power and LCAR concentration during absorption.

Absorber Bed Stability and Design Improvements. When the LiCl solution approaches its final concentration (typically < 50%), it enters a fully liquid phase. In this condition, the liquid solution is free to flow through the sponges that comprise the solid structure of the bed. During operation, vapor flow across the LCAR gives rise to a pressure gradient of about 1 torr (133 Pa). This is equivalent to a head difference of about 0.5 in. of water, and is large enough to drive a small flow of solution from the high-pressure (vapor inlet) to the low-pressure (capillary vent) side of the LCAR. When the LCAR is regenerated, the extra solution near the capillary vent tends to leave additional solid LiCl behind. Since our past practice has been to test the LCAR in the same orientation every time, this effect can build up over the course of multiple absorption/regeneration cycles. We believe this can lead to formation of small salt plugs near the LCAR exit that are not in good communication with water vapor during absorption because their physical dimensions are too large for water to diffuse in during the course of an absorption run. This effect would be greatly amplified if gravitational forces drive the liquid flow, and we have found that storing an LCAR vertically before regeneration can lead to a very significant rearrangement of the internal solution inventory. We do not yet know whether vertical storage has a large effect on absorption performance.

One way to stabilize the solution inventory is to add hydrophobic structures to the absorber bed that prevent the liquid from moving very far. Our current plans are to build an LCAR with appropriate, internal capillary structures and compare its performance with earlier prototypes without the new structures.

X. Conclusions and Future Directions

Recent developments in LCAR technology have demonstrated the ability to build multiple LCAR panels with consistent absorption and regeneration behavior, as well as indicating areas for additional work to improve the consistency of performance from run to run. The main conclusions based on recent findings are:

- State-of-the-art absorber bed designs have boosted LCAR operating temperature by about 10°C compared to prior designs.
- LCAR performance is generally stable and repeatable across several absorption/regeneration cycles and between different units.
- Small differences in performance from run to run are probably due to migration of liquid LiCl/water solution due to pressure gradients inside the LCAR.
- The LCAR structure is extremely rugged and durable, able to survive design-basis impact tests and extreme overpressurization (10× MEOP) without losing LiCl containment.
- No change in the LCAR's thermal performance can be observed following a design-basis impact test.
- The characteristics of LCAR performance can be attributed to the complex phase behavior of the LiCl/water system.

In addition, parallel efforts under way at UTAS have assessed various candidate SEAR coolants and concluded that deionized water with elemental iodine, operating in a manner similar to the EMU ALCLR system, has good potential for use in the SEAR system. Testing shows that the iodine will vaporize in the SWME and condense in the LCAR, but the expected concentrations of iodine should have negligible impact on LCAR performance.

Ongoing and future work will focus on improving consistency of LCAR performance and boosting the technology readiness level to enable future flight tests. This includes the following:

- Improvements to absorber bed design to limit motion of liquid solution due to pressure gradients.

- Demonstration of stable operation using improved designs
- Flight qualification of prototype LCAR units.
- Assembly and qualification of a flight-like regeneration oven.
- Quantification of the behavior of iodine in LCAR, including effects on absorption performance and whether the concentration builds up over time.
- Design of prototype LCAR panels that can be used as structural elements for a PLSS backpack.

Acknowledgments

The authors gratefully acknowledge the support of NASA Lyndon B. Johnson Space Center and the NASA SBIR program.

References

[1]Bue, G., Hodgson, E., Izenson, M., and Chen, W. "Multifunctional Space Evaporator-Absorber-Radiator," Presented at: 43rd International Conference on Environmental Systems (ICES), AIAA 2013-3306, Vail, CO, 14–18 Jul 2013.

[2]Izenson, M. G., Phillips, S. D., Chepko, A. B., Quinn, G., Steele, J. and Bue, G., "Design of a Lithium Chloride Absorber Radiator for Flight Testing on an Extravehicular Mobility Unit," Presented at: 46th International Conference on Environmental Systems (ICES), Vienna, Austria, ICES-2016-232, 10–14 Jul 2016.

[3]Hodgson, E., Izenson, M., Chen, W., and Bue, G., "Spacesuit Evaporator-Absorber-Radiator (SEAR)," Presented at the 42nd International Conference on Environmental Systems, July 2012, San Diego, CA AIAA 2012-3484.

[4]Monnin, C., Dubois, M., Papaiconomou and Simonin, J.-P., "Thermodynamics of the LiCl + H_2O System," *J. Chem. Eng. Data,* Vol. 47, No. 6, 2002, pp. 1331–1336.

[5]Rau, J. J., "Thermodynamic Characteristics of Lithium Chloride in Rotary Heat and Mass Exchangers," M.S. Thesis, Department of Chemical Engineering, University of Wisconsin-Madison, 1989.